

# Special Article

## Scintigraphic appearance of selected diseases of the equine head

D. C. ARCHER\*, C. L. BLAKE, E. R. SINGER, J. C. BOSWELL<sup>†</sup>, J. C. COTTON, G. B. EDWARDS AND C. J. PROUDMAN

*Philip Leverhulme Large Animal Hospital, University of Liverpool, Leahurst, Neston, Wirral CH64 7TE and <sup>†</sup>The Liphook Equine Hospital, Forest Mere, Liphook, Hampshire GU30 7JG, UK.*

**Keywords:** horse; gamma scintigraphy; dental disease; sinusitis; disease of head

### Introduction

Diagnosis of disease of the head is usually based on patient history, clinical examination and the use of ancillary diagnostic aids. Endoscopy is frequently used to visualise the upper airways, but direct access into the paranasal sinuses is not possible in the normal horse. Sinoscopy provides a more invasive means of examining the internal structure of the paranasal sinuses (Ruggles *et al.* 1993; Beard and Hardy 2001). Radiography is commonly used to evaluate the head, but the complex internal structure results in superimposition of multiple opacities which can make radiological interpretation difficult, particularly in the evaluation of the nasal passages, teeth, paranasal sinuses and temporomandibular joint (Metcalf *et al.* 1989). Although radiography is highly specific for dental disease, it is of low sensitivity (Gibbs and Lane 1987; Weller *et al.* 2001). Other imaging methods include computed tomography and magnetic resonance imaging, which provide high resolution images of all areas of the head such as the brain (Tietje *et al.* 1996; Tucker and Farrell 2001). However, for these two techniques, general anaesthesia is required to obtain the images. Image acquisition and interpretation also require specialist expertise and equipment.

**Scintigraphic examination of the head has been shown to be a useful adjunctive imaging modality in the horse** (Metcalf *et al.* 1989). Most reports have described the use of scintigraphy in the evaluation of dental disease (Boswell *et al.* 1999; Gayle *et al.* 1999; Semevolos *et al.* 1999; Weller *et al.* 2001), but few reports have described the scintigraphic features of other pathological diseases of the head (Walmsley 1988; Metcalf *et al.* 1989; Weller *et al.* 1999; Stadtbäumer and Boening 2002). We have previously described the normal scintigraphic appearance of the head (Archer *et al.* 2002). This paper describes the scintigraphic appearance of selected diseases of the equine head.

### Materials and methods

Nineteen horses were presented to the Philip Leverhulme Large Animal Hospital or The Liphook Equine Hospital for investigation of abnormalities of the head. All horses underwent a full clinical examination including oral examination. Endoscopy of the nasal passages, pharynx and guttural pouches was performed in each case. Lateral and oblique radiographs of the head were obtained. Dorsal 30° lateral oblique views were performed in horses with suspected disease of the maxillary cheek teeth and ventral 45° lateral oblique views in those with suspected disease of the mandibular cheek teeth. Further lateral oblique and dorsoventral views were obtained as necessary to highlight particular regions.

### Technique

Via an indwelling jugular catheter, 10 MBq/kg bwt <sup>99m</sup>technetium methylenediphosphonate (<sup>99m</sup>Tc-MDP) was given. Bone phase images were acquired 3–4 h after injection of radioisotope in each horse. Soft tissue phase images were obtained in one horse 5–15 mins after administration of radioisotope.

All horses were sedated i.v. with 0.04 mg/kg bwt romifidine or 0.01 mg/kg bwt detomidine and 0.01 mg/kg bwt butorphanol. The horses were restrained in stocks and a rope halter applied. In most cases, cotton wool was used to plug the ears, to reduce auditory stimuli, and blinkers were applied. A stool was used to stabilise the patient's head, preventing rotation in the sagittal plane.

### Image acquisition

Images were obtained using a GE 400A Analog Autotune System gamma camera with a 12.5 mm NaI (T1) Harshaw crystal and 61 RCA photomultipliers interfaced with a dedicated nuclear medicine computer<sup>1</sup>. Images were acquired

\*Author to whom correspondence should be addressed.

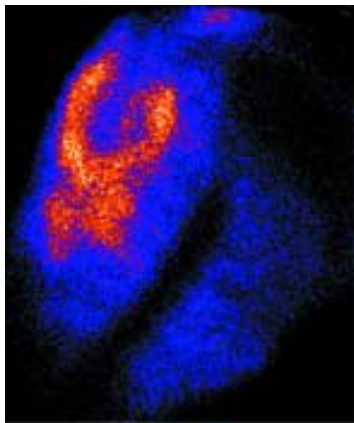


**Fig 1:** Lateral image demonstrating a 'C'-shaped uptake of radioisotope in the paranasal sinuses of a horse with unilateral primary sinusitis (Horse 5).

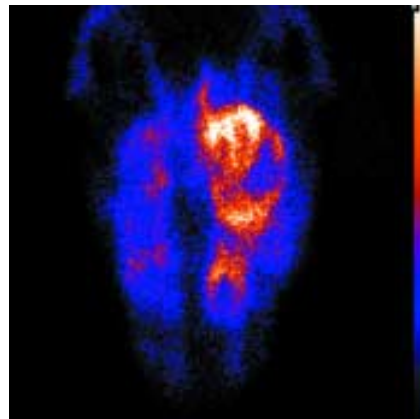


**Fig 3:** Dorsal view in a horse with unilateral sinusitis demonstrating patchy increased uptake of radioisotope in the paranasal sinuses (Horse 4). This view enables easy differentiation between unilateral and bilateral sinusitis.

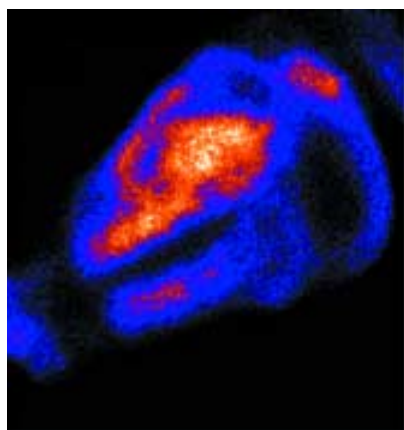


**Fig 2:** Lateral image demonstrating diffuse uptake of radioisotope in the maxillary and frontal sinuses in a pony with bilateral primary sinusitis (Horse 3).

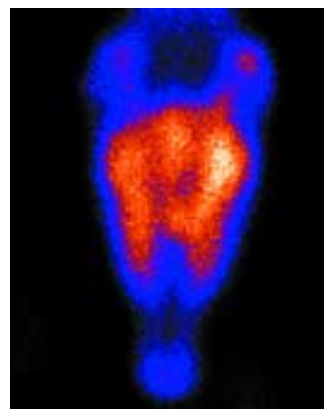


**Fig 4:** Dorsal view of the head in Horse 3 (diagnosis of bilateral primary sinusitis) demonstrating diffuse increased uptake of radioisotope in the left and right paranasal sinuses.

dynamically as 60 consecutive 2-second frames. Right lateral, left lateral, dorsal and ventral views were obtained for each head using a 50 cm field of view parallel hole collimator.

Regions of interest (ROIs) were created around specific structures in the head using a multimodality programme, allowing the counts for a ROI to be compared with the corresponding area on the opposite side of the head. The difference between counts on each side was expressed as a percentage. When bilateral disease was present, ratios were used to determine the amount of radioisotope uptake (RU) in the area of interest compared to a set reference point. The reference point used in this study was the body of the vertical ramus of the mandible. The calculated ratio was then compared to that of a normal horse (Archer *et al.* 2003).

## Results

### Animals

Details of the horses used in this study are shown in **Table 1**. Clinical details and results of diagnostic tests are shown in **Table 2**.

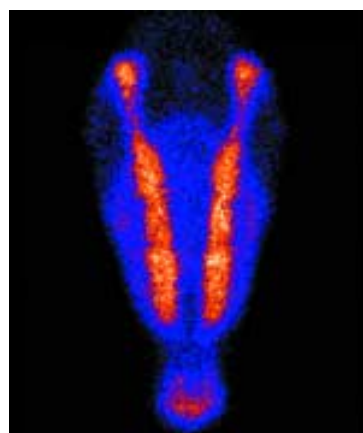


**Fig 5:** Ventral view of the head in Horse 3. Note the small uptake of radioisotope in the maxillary sinuses lateral to the cheek teeth on this view.

### Primary sinusitis

In cases of primary sinusitis, the patterns of RU on the lateral views varied from an incomplete circular area to diffuse

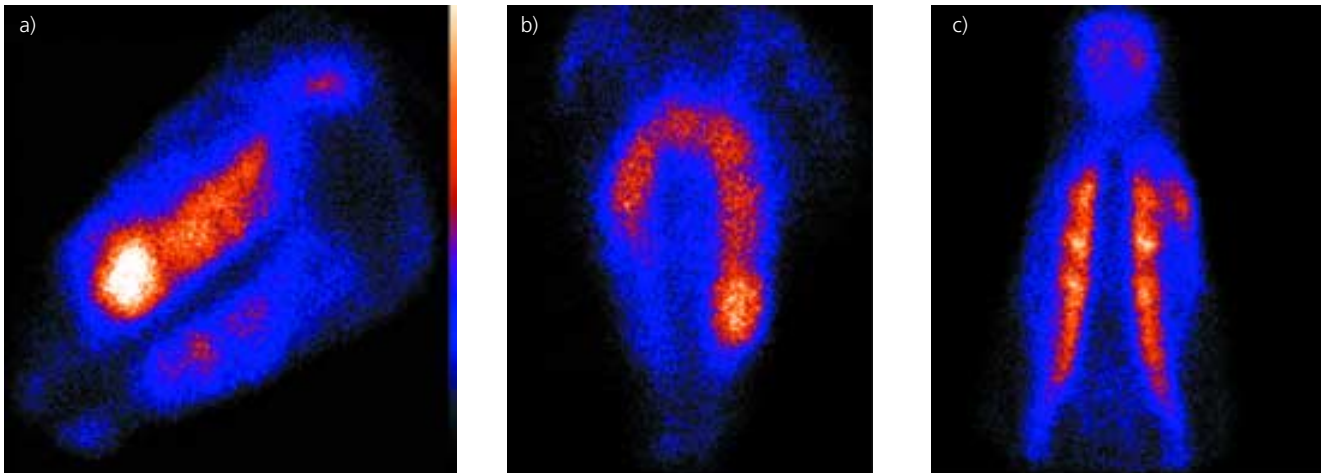


**Fig 6:** Images obtained in Horse 10. *a)* The left lateral image demonstrates increased uptake of radioisotope in the alveolar bone of the 2nd maxillary cheek tooth. *b)* The dorsal image allows the affected side to be determined easily. *c)* The ventral image demonstrates increased uptake of radioisotope in the adjacent maxillary bone.

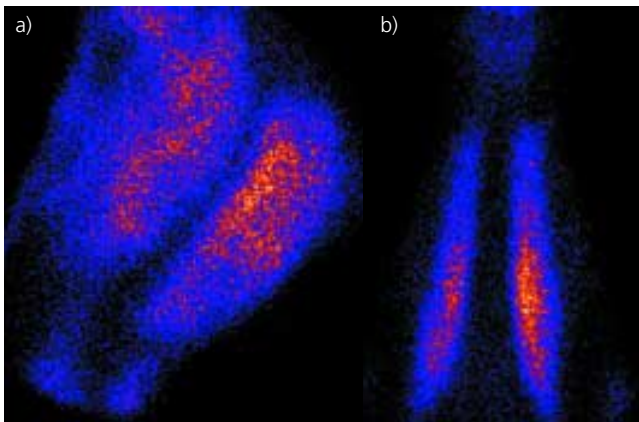


**Fig 7:** Diffuse uptake of radioisotope in the interdental bone of the caudal mandibular cheek teeth in Horse 11 on *a)* lateral and *b)* ventral views.

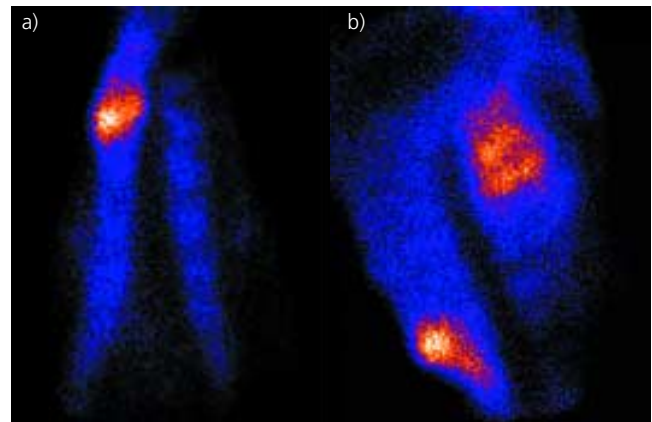


**Fig 8:** *a)* Ventral and *b)* right lateral images obtained in Horse 12 demonstrating focal, increased uptake of radioisotope around the 1st right mandibular cheek tooth.

increased radioisotope uptake (IRU) in all the paranasal sinuses (**Figs 1** and **2**). It was possible to distinguish the maxillary and frontal sinuses based on anatomical location. The interdental and alveolar bone of the dental arcades was evident, but showed less RU than in the sinuses. Uptake of radioisotope on one side of the head may be seen on the contralateral image. We have termed this 'strike through'. When unilateral sinusitis was present, some 'strike through' was evident on the contralateral image, but the affected side always showed greater uptake. The dorsal view showed variable patterns of RU, from diffuse to patchy (**Figs 3** and **4**). The dental arcades were indistinct on this view. The dorsal view was most useful to confirm the presence of unilateral or bilateral sinusitis. The mandibular dental arcades were clearly outlined on the ventral view. Small to moderate quantities of RU were present in the maxillary bone, lateral to the dental arcades (**Fig 5**). When unilateral sinusitis was present, IRU in the maxillary sinus was evident on the affected side. Trephination of the paranasal sinuses had been performed 4–6 weeks prior to scintigraphy

in 2 horses, but there was no marked difference between images obtained in these horses compared to the others. Duration of the disease process did not appear to affect the pattern of uptake. In horses with unilateral sinusitis, ROI studies performed on the dorsal images demonstrated 68–93% greater RU in the affected sinus compared to the contralateral sinus.

#### **Dental disease without sinusitis**

Periapical infection resulted in marked, focal IRU over the affected tooth root (**Fig 6a**). The lateral views were the most useful to allow accurate identification of the affected tooth. Accurate identification was facilitated by obtaining good images and was easiest in younger horses. ROIs were most easily performed on the dorsal views where maxillary cheek teeth were involved or on the ventral views with mandibular cheek tooth involvement (**Fig 6b**). ROI studies performed on the appropriate dorsal or ventral images showed that the

**TABLE 1: Age, breed and sex of clinical cases used in this study**

		No. clinical cases (n = 19)
Breed	Thoroughbred /TB x	9
	Arab x	1
	Warmblood	1
	Pony	5
	Shire	1
	Cob	1
	Hunter	1
Sex	Mares	10
	Geldings	9
Age	12 months–20 years (median 8 years )	19

affected regions had 61–120% greater RU compared to the same region on the contralateral side. In 2 horses with periapical infection of one of the rostral 3 maxillary cheek teeth, it was possible to identify a subtle increase in RU in the adjacent maxillary bone on the ventral views (**Fig 6c**).

Localised periodontal disease (*Horse 11*) was identified as a subtle, diffuse increase in RU in the interdental bone of the affected area (**Figs 7a,b**). ROI studies showed a 50% increase in counts in the affected area compared to the contralateral side on the ventral view.

*Horse 12* showed focal, marked IRU in the region of the root of the first mandibular cheek tooth (**Figs 8a,b**). ROI studies on the ventral image showed 171% greater uptake in the alveolar bone at this site compared to the same region on the contralateral side. ‘Strike through’ was apparent on the lateral view on the unaffected side, with higher counts being detected on the affected side. The ventral view was the most useful to identify which tooth was affected. The dorsal view revealed an increased uptake of radioisotope in the region, but it was not possible to identify its location accurately.

### **Sinusitis secondary to dental disease**

In horses with sinusitis secondary to dental disease, variable patterns of RU were evident in the sinuses on the lateral views. Generally, the areas of RU were more focal around the region of the affected tooth compared to the patterns of uptake in horses with primary sinusitis (**Fig 9a**). ‘Strike through’ pattern was present in the lateral images of the nonaffected side of the head, but lateral images of the affected side always showed greater RU over the affected sinuses and tooth root (**Fig 9b**). Focal IRU was evident in the alveolar bone surrounding the affected tooth. The dorsal views revealed less diffuse patterns of uptake over the sinus regions compared to the images obtained in horses with primary sinusitis. The dental arcades were well outlined but it was not possible accurately to localise the affected tooth on the dorsal view (**Fig 9c**). The ventral views showed IRU associated with the maxillary sinus on the affected side. Again, it was not possible to identify the affected maxillary cheek tooth on this view.

### **Mandibular abscess**

Soft tissue phase images were obtained in one horse with a mandibular abscess. These images showed a diffuse ‘C’-shaped increase in RU in the soft tissues around the affected mandibular ramus on the ventral and lateral views (**Figs 10a,b**). On the ventral bone phase image, there was a thin, linear increase in RU in the ramus of the mandible (**Fig 10c**). There was an 86% higher uptake of radioisotope in the affected mandibular ramus compared to the ramus of the contralateral mandible on the bone phase image, despite slight rotation of the image. The lateral and dorsal views were not useful to demonstrate the lesion.

### **Adenocarcinoma**

The right and left lateral views of *Horse 19* demonstrated intense, diffuse IRU in the maxillary and frontal sinuses (**Fig 11b**). The counts were greatest on the lateral view on the affected side, but a similar, less intense and clearly defined pattern of uptake was evident on the contralateral image. A circular, focal pattern of increased uptake was evident in the affected maxillary sinus on the ventral view. On the dorsal view, a diffuse pattern of IRU was evident in both maxillary and frontal sinuses, being most intense on the clinically affected side of the head (**Fig 11a**). Ratios were determined by comparing the counts from the affected sinuses to the body of the mandible. When compared to the ratios determined from the same areas in a similarly aged horse with no clinical evidence of disease, levels of uptake were 300–400% higher.

### **Other findings**

In *Horse 11*, there was a disparity in the appearance of the temporomandibular joints (TMJ) (**Fig 12**). ROI studies performed on the dorsal image showed a 20% difference between the 2 sides. However, this was thought to be caused by rotation of the image.

In *Horse 8*, an area of unilateral increased uptake was noted on the ventral and lateral views in the region of the 5th mandibular cheek tooth (**Fig 13**), although there was no evidence of pathology on physical examination and radiography.

*Horse 13* was diagnosed with a possible periapical infection based on clinical signs and radiography. Scintigraphy revealed a normal appearance of the head. ROIs applied to the area around the 2nd maxillary cheek teeth revealed no significant difference between the two sides. No treatment was undertaken and the facial swelling resolved over a period of several weeks.

### **Discussion**

This study illustrates the scintigraphic appearance of selected diseases of the equine head. Scintigraphy appears to be helpful to differentiate horses with primary sinusitis from those

**TABLE 2: Relevant history, clinical findings, diagnosis and outcome in 19 horses with disease of the head**

Horse (years)	Age	History and clinical signs	Diagnostic imaging	Diagnosis	Response to treatment
1	3	Bilateral mucopurulent ND	Rad: fluid lines in L&R RMS	Bilateral primary sinusitis	Resolution after trephination and flushing of sinus
2	14	3 month duration R mucopurulent ND	Endo: purulent discharge R maxillary drainage angle Rad: fluid lines R RMS & CMS	Unilateral primary sinusitis	Resolution following surgical debridement and lavage
3	1	Bilateral L>R mucopurulent ND	Rad: radiopacity of L&R RMS, CMS and FS	Bilateral primary sinusitis	Resolution after trephination and flushing
4	8	L nasal discharge, upper respiratory noise at exercise, L epiphora	Endo: swollen and inflamed L conchae Rad: fluid lines L RMS & CMS	Unilateral primary sinusitis	Resolution following surgical debridement
5	4	L purulent ND. Firm swelling over L RMS	Endo: L ethmoturbinate distortion and distension dorsal concha Rad: radiopacity within L CMS	Unilateral chronic sinusitis	Resolution with surgical debridement and flushing
6	12	Difficulty masticating food R side of mouth, Fracture of R 3rd mandibular CT identified on intra-oral examination	Rad: longitudinal fracture R 3rd mandibular CT	Fractured 3rd R mandibular CT	Resolution following extraction 3rd R mandibular CT
7	8	6 week history of development of firm swelling rostral to R facial crest	Rad: sclerosis and periapical lucency around apices of R 2nd maxillary CT	Periapical infection R 2nd maxillary CT	Resolution following extraction R 2nd maxillary CT
8	2	Firm swelling over L facial crest with central discharging sinus of purulent material	Rad: sclerosis, truncation of apices, cementosis, loss of lamina dura around L 3rd and 4th maxillary CT	Periapical infection L 4th maxillary CT	No treatment undertaken at owner's request
9	4	Firm swelling over L facial crest	Rad: loss of lamina dura around L 3rd maxillary CT, sclerosis alveolar bone and overlying soft tissue density	Periapical infection L 3rd maxillary CT	Resolution of signs following extraction L 3rd maxillary CT
10	10	2 month history of firm swelling rostral to L facial crest	Rad: loss of lamina dura around L 2nd maxillary CT, sclerosis alveolar bone	Periapical infection L 2nd maxillary CT	Resolution following extraction L 2nd maxillary CT
11	6	5 week history of quidding, sharp enamel points on upper and lower arcades. Diastema between L 5th and 6th mandibular CT containing food material	Rad: diastema	Periodontal disease around 5th mandibular CT	No treatment other than rasping of teeth undertaken
12	6	Smooth, osseous mass over rostral aspect R mandible	Rad: remodelling of ventral mandible, periapical lysis of caudal root of R 1st mandibular CT	Possible early apical abscess/trauma	Resolution without further treatment
13	10	Smooth, firm mass rostral to facial crest L side face	Rad: periapical radiolucency around rostral root 2nd L maxillary CT and sclerosis adjacent maxillary bone	Possible apical abscess L 2nd maxillary CT	Resolution without further treatment
14	16	L ND	Rad: soft tissue density L RMS and CMS, loss of lamina dura around L 4th and 5th maxillary cheek teeth	Dental sinusitis	Resolution following repulsion L 4th maxillary CT
15	20	R-sided malodorous ND, firm swelling over R RMS, R epiphora	Rad: fluid lines L CMS, periapical radiolucency R 5th maxillary CT, ill defined roots L and R 4th maxillary CT	Dental sinusitis	Resolution after repulsion L 4th maxillary CT
16	8	R ND, food material impacted in R 5th maxillary CT	Rad: fluid line in R RMS, periapical sclerosis R 4th and 5th maxillary CT	Dental sinusitis	Resolution after repulsion of R 5th maxillary CT
17	6	R mucopurulent ND (4 months)	Rad: generalised radiopacity CMS, RMS and FS, irregularity of lamina dura caudal root right 3rd CT	Dental sinusitis	Resolution following extraction R 3rd CT, debridement and lavage R paranasal sinuses
18	15	Acute onset dysphagia, salivation, weight loss. Pain and soft tissue swelling over caudomedial aspect L mandible	US: mass with hyperechoic capsule and hypoechoic centre	Mandibular abscess	Resolution following surgical debridement of abscess
19	10	R-sided exophthalmos, epiphora, ND and facial swelling	Endo: dorsal compression R guttural pouch and dorsal concha Rad: soft tissue radiodensity R RMS, CMS and FS	Adenocarcinoma of paranasal sinuses	Euthanasia after confirmation by biopsy

R = right; L = left; CT = cheek tooth; ND = nasal discharge; Rad = radiology; Endo = endoscopy; US = ultrasound; RMS = rostral maxillary sinus; CMS = caudal maxillary sinus; FS = frontal sinus.

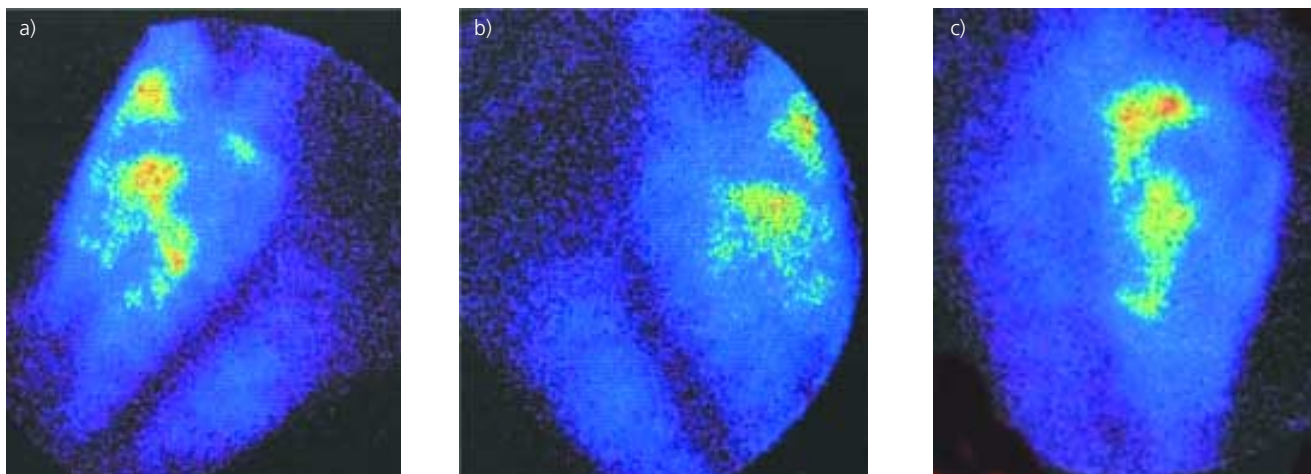


**Fig 9:** a) Left lateral image in Horse 14 demonstrating uptake of radioisotope in the alveolar bone of the 4th maxillary cheek tooth and patchy uptake in the paranasal sinuses. b) Some 'strike-through' is evident on the right lateral image, but the quantity of radioisotope uptake is higher on the affected side. c) The dorsal view enables the affected side to be determined easily but it is difficult to accurately localise the specific tooth on this view.

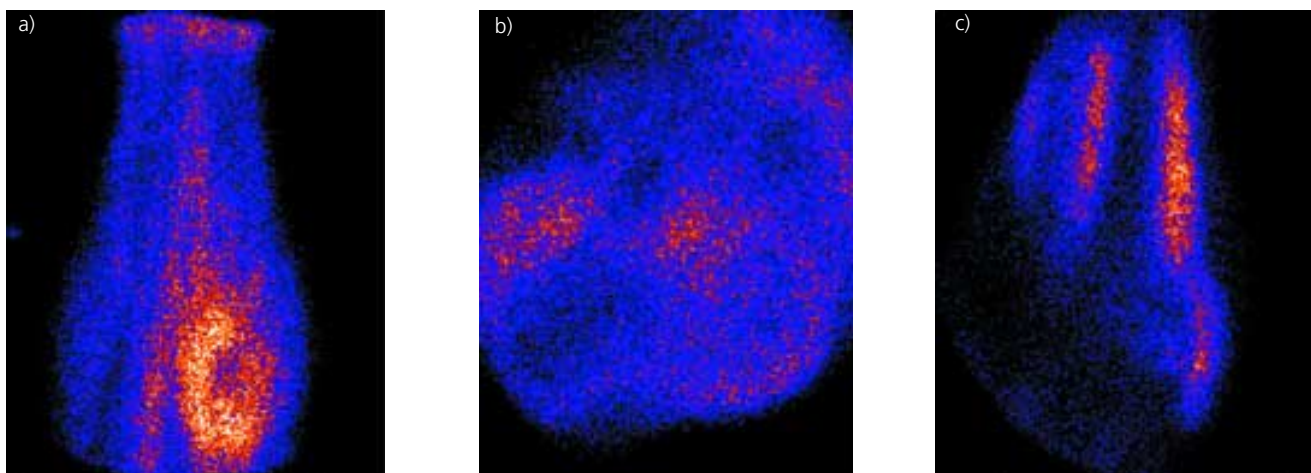


**Fig 10:** a) Ventral and b) left lateral soft tissue phase images obtained in Horse 18. c) The ventral bone phase image demonstrates a thin area of increased radioisotope uptake in the ventral mandible. Slight rotation of this image has occurred.

with sinusitis secondary to dental disease. It is a low resolution, high sensitivity imaging technique and, when used alone, offers no particular advantage over radiography in identifying which tooth is involved in dental disease. However, when used in conjunction with radiography, it improves the probability of accurately identifying the affected tooth (Weller *et al.* 2001). Diseases that mainly affect soft tissue (e.g. abscesses, periodontal disease, adenocarcinoma) can be difficult to characterise radiographically but demonstrate characteristic scintigraphic changes.

The scintigraphic appearance of equine dental disease has been documented previously (Metcalf *et al.* 1989; Boswell *et al.* 1999; Gayle *et al.* 1999; Semevolos *et al.* 1999; Weller *et al.* 2001). The appearance of periapical infection in this study was consistent with previous reports. Weller *et al.* (2001) stated that a ratio of greater than 1.5 between a suspected tooth and the contralateral tooth resulted in a false positive rate of 1% and false negative rate of 20% in the diagnosis of

periapical infection. This corresponds well with the results of regions of interest measurements performed in this study. Localised osteitis is a feature of chronic periapical infection, particularly in the rostral maxillary cheek teeth (Gibbs 1995). This finding was detected in several cases in this study, particularly on the ventral views.

Periapical infection was suspected in *Horse 12* and gamma scintigraphy confirmed increased metabolic activity in the affected region, suggestive of this disease process. No treatment was undertaken at the time and the bony swelling progressively reduced. Spontaneous resolution may occur in cases of periapical infection in young horses (G.B. Edwards, personal communication), or increased uptake may have been secondary to trauma to the affected area of the mandible in this case.

The present study suggests that periapical infection is likely to be identified easily using scintigraphy after injection of  $^{99m}\text{Tc}$ -MDP. However, in some horses, more than one tooth may be associated with IRU, making diagnosis of the affected tooth

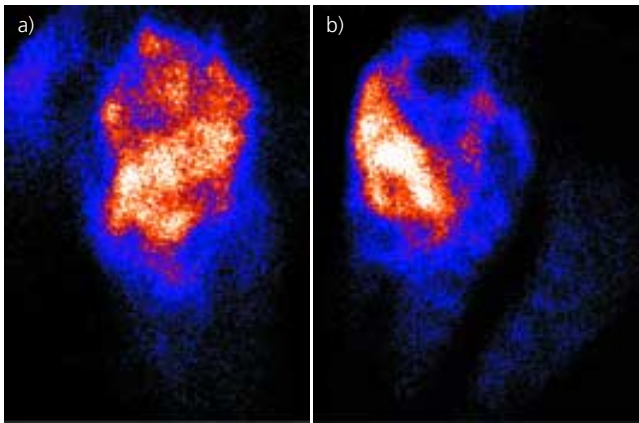


**Fig 11: a) Dorsal and b) left lateral images obtained in Horse 19 demonstrating marked increase of radioisotope in the paranasal sinuses. Some rotation has occurred in (a).**

more difficult. It has been suggested that the use of scintigraphy after re-injection of HMPAO-labelled leucocytes (Boswell *et al.* 1999) may provide useful adjunctive information in some horses. This technique may also have had some application in *Horse 13*, where no abnormal scintigraphic findings were detected on bone phase images. Scintigraphy may be useful to rule out dental disease where there are equivocal clinical or radiographic signs, thereby avoiding unnecessary tooth removal (Semevolos *et al.* 1999) or to rule out root involvement where fracture has occurred (Metcalf *et al.* 1989). Weller *et al.* (2001) reported negative scintigraphic findings to be more reliable than radiography in ruling out the presence of periapical infection.

Periodontal disease has been shown to cause IRU in the interproximal (interdental) bone of multiple teeth, resulting in a linear pattern of activity over the affected arcade (Boswell *et al.* 1999; Weller *et al.* 2001). The appearance of a linear pattern of uptake in these cases rather than a string of 'hot spots' suggests that there is a generalised increase in uptake in the upper alveolar bone as well, rather than just the interproximal bone. Periodontal disease occurs with increasing frequency in horses over age 16 years (Baker 1970). This may make differentiation between normal age-related changes in the appearance of the arcades and subclinical periodontal disease in older horses difficult; however, the typical clinical signs and intra-oral findings should allow identification of periodontal disease. Alternatively, ratios of radioisotope uptake between horses of similar ages allow quantification of changes to be made and compared. Localised periodontal disease may be secondary to developmental abnormalities such as diastema, as was found in *Horse 11*. The scintigraphic findings were consistent with a localised, low-grade reactive process in the osseous structures surrounding the affected tooth.

Soft tissue phase images were obtained in only one horse in this study. Because these images must be obtained 10–15 mins after radioisotope administration (Martinelli and Chambers 1995), it can be difficult to obtain a complete set of comparable images during this time and it increases the quantity of radiation to which personnel are exposed. Weller *et al.* (2001) described the normal appearance of the soft tissue

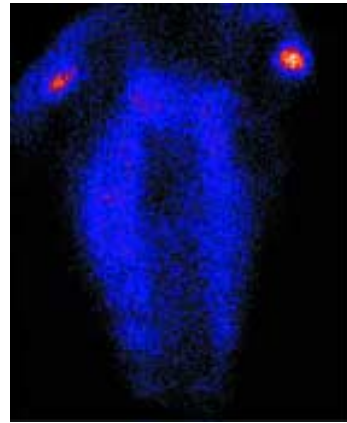


**Fig 12: Dorsal view obtained in Horse 11 demonstrating asymmetric uptake of radiopharmaceutical in the temporomandibular joint. However, slight rotation of the image has occurred, demonstrated by the asymmetrical appearance of the maxillary dental arcades.**

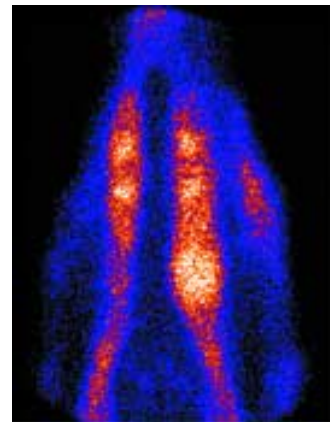


**Fig 13: Ventral view obtained in Horse 8 demonstrating increased radioisotope uptake in the left maxillary bone and alveolar bone of the 5th mandibular cheek tooth. The latter may be related to eruption of the permanent tooth at this site in this 2-year-old horse.**

phase images of the head. These images did not provide any additional information to the bone phase images in cases of dental disease in their study and were consistent with the findings in the mandibular abscess case presented in this study.

Primary or secondary sinusitis is the most frequent cause of equine sinonasal disease (Tremaine and Dixon 2001). Differentiation between primary and dental sinusitis can be difficult to determine radiographically (Gibbs and Lane 1987; Tremaine and Dixon 2001). Diagnosis may be based on the response to treatment of primary sinusitis (Dixon *et al.* 2000). In this study, scintigraphy allowed differentiation between primary and dental sinusitis. The patterns of uptake are consistent with those noted in similar groups in other studies (Metcalf *et al.* 1989; Boswell *et al.* 1999; Semevolos 1999).

Sinonasal neoplasia is uncommon in the horse (Tremaine and Dixon 2001). Most tumours originate in the paranasal sinuses, and nonspecific signs of nasal discharge or facial swelling may have been present for variable periods of time prior to diagnosis

(Dixon and Head 1999). Adenocarcinomas have been reported previously to originate from the frontal sinus, nasal or ethmoidal regions (Head and Dixon 1999). Radiography often does not allow differentiation to be made between true neoplasms and the more commonly occurring non-neoplastic sinonasal masses. Sinoscopy may be impeded by the size of the mass and secondary empyaema. Surgical exploration may be limited, depending on the origin of the neoplasm. The scintigraphic images obtained in the case presented here were consistent with a diffuse, aggressive disease process resulting in distortion of the normal image of the paranasal sinuses. Most sinonasal neoplasms carry a poor prognosis, due to their advanced stage by the time of diagnosis (Dixon and Head 1999). Early diagnosis is critical to a potentially successful outcome with the more recently developed therapeutic options such as radiotherapy (Walker *et al.* 1998; Baker 1999). Therefore, gamma scintigraphy may offer an additional imaging modality for the early detection of these cases.

Temporomandibular joint (TMJ) disease may arise secondary to dental pathology due to the alterations in jaw movement during mastication (Knottenbelt 1999). This could explain the difference in appearance between the TMJs in *Horse 11*. However, the differences in uptake were not marked and more probably were due to rotation of the dorsal image. Care must be exercised with interpretation of equivocal differences in uptake in the TMJ, particularly when the image is not perfectly symmetrical. Confirmation of TMJ pathology should be based on intra-articular anaesthesia, ultrasonography or arthroscopy (Weller *et al.* 1999; May *et al.* 2001). Metcalf *et al.* (1989) reported the use of follow-up scintigraphy to confirm reduction in TMJ inflammation subsequent to resolution of the inciting cause.

The normal eruption of teeth and the radiographic changes in appearance of cheek teeth with age are well documented (Dixon and Copeland 1993). The scintigraphic appearance of the mandibular arcades in *Horse 8* (Fig 13), a 2-year-old, may have been related to normal eruption of the 5th cheek tooth. Further studies need to be performed to determine the scintigraphic changes associated with normal eruption of cheek teeth.

Gamma scintigraphy is a useful imaging modality in the investigation of disease of the head. Its use should be considered when more commonly utilised imaging modalities have proven equivocal or inconclusive. It may be most useful clinically to assist differentiation between sinusitis of primary or dental origin. Gamma scintigraphy is a valid screening tool where nonspecific signs of disease of the head are present and may allow earlier detection of disease processes which require prompt and aggressive treatment.

## Acknowledgements

This study was funded by Petplan Charitable Trust. Debra Archer is partially funded by the Clarke and Sparrow RCVS trust. Caroline Blake was a Home of Rest for Horses resident in Equine Soft Tissue Surgery. Technical assistance by S. Bloomer, Nuclear Diagnostics is gratefully acknowledged.

## Manufacturer's address

<sup>1</sup>Nuclear Diagnostics AB, Hägersten, Sweden.

## References

- Archer, D.C., Blake, J.C., Singer, E.R., Boswell, J.C., Cotton, J.C., Edwards, G.B. and Proudman, C.J. (2003) The normal scintigraphic appearance of the equine head. *Equine vet. Educ.* **35**, 243-249.
- Baker, G.J. (1970) Some aspects of equine dental disease. *Equine vet. J.* **2**, 105-110.
- Baker, G.J. (1999) Equine nasal and paranasal tumours. *Vet. J.* **157**, 220-221.
- Beard, W.L. and Hardy, J. (2001) Diagnosis of conditions of the paranasal sinuses in the horse. *Equine vet. Educ.* **13**, 265-273.
- Boswell, J.C., Schramme, M.C., Livesey, L.C. and Butson, R.J. (1999) Use of scintigraphy in the diagnosis of dental disease in four horses. *Equine vet. Educ.* **11**, 294-298.
- Dixon, P.M. and Copeland, A.N. (1993) The radiological appearance of mandibular cheek teeth in ponies of different ages. *Equine vet. Educ.* **5**, 317-323.
- Dixon, P.M. and Head, K.W. (1999) Equine nasal and paranasal sinus tumours: Part 2: a contribution of 28 case reports. *Vet. J.* **157**, 279-294.
- Dixon, P.M., Tremaine, W.H., Pickles, K., Kuhns, L., Hawe, C., McCann, J., McGorum, B.C., Railton, D.I. and Brammer, S. (2000) Equine dental disease Part 4: a long-term study of 400 cases: apical infections of cheek teeth. *Equine vet. J.* **32**, 182-194.
- Gayle, J.M., Redding, W.R., Vacek, J.R. and Bowman, K.F. (1999) Diagnosis and surgical treatment of periapical infection of the third mandibular molar in five horses. *J. Am. vet. med. Ass.* **215**, 829-832.
- Gibbs, C. (1995) Radiography of the head and soft tissue structures of the neck. *Equine vet. Educ.* **7**, 324-348.
- Gibbs, C. and Lane, J.G. (1987) Radiographic examination of the facial nasal and paranasal sinus regions of the horse II. Radiological findings. *Equine vet. J.* **19**, 474-482.
- Head, K.W. and Dixon, P.M. (1999) Equine nasal and paranasal sinus tumours. Part 1: review of the literature and tumour classification. *Vet. J.* **157**, 261-278.
- Knottenbelt, D.C. (1999) The systemic effects of dental disease In: *Equine Dentistry*, Eds: J.G. Baker and J. Easley, W.B. Saunders Co., Philadelphia. pp 129-130.
- Martinelli, M.J. and Chambers, M.D. (1995) Equine nuclear bone scintigraphy: physiological principles and clinical application. *Equine vet. Educ.* **7**, 281-287.
- May, K.A., Moll, H.D., Howard, R.D., Pleasant, R.S. and Gregg, J.M. (2001) Arthroscopic anatomy of the equine temporomandibular joint. *Vet. Surg.* **30**, 564-571.
- Metcalf, M.R., Tate, L.P. and Sellett, L.C. (1989) Clinical use of <sup>99m</sup>Tc-MDP scintigraphy in the equine mandible and maxilla. *Vet. Radiol.* **30**, 80-87.
- Ruggles, A.J., Ross, M.W. and Freeman, D.E. (1993) Endoscopic examination and treatment of paranasal sinus disease in the horse. *Vet. Surg.* **22**, 508-514.
- Semevolos, S.A., Hackett, R.P. and Scrivani, P.V. (1999) Nuclear scintigraphy as a diagnostic aid in the evaluation of tooth root abscessation. *Proc. Am. Ass. equine Practnrs.* **45**, 103-104.
- Stadtbäumer, G. and Boening, K.J. (2002) Diagnostische und arthroskopische Verfahren am Kiefergelenk des Pferdes. *Tierärztl. Prax.* **30**, 99-106.
- Tietje, S., Becker, M. and Böckenhoff, G. (1996) Computed tomographic evaluation of head diseases in the horse: 15 cases. *Equine vet. J.* **28**, 98-105.

- Tremain, W.H. and Dixon, P.M. (2001) A long-term study of 277 cases of equine sinonasal disease. Part 1: Details of horses, historical, clinical and ancillary diagnostic findings. *Equine vet. J.* **33**, 274-282.
- Tucker, R.L. and Farrell, E. (2001) Computed tomography and magnetic resonance imaging of the equine head. *Vet. Clin. N. Am.: Equine Pract.* **17**, 131-144.
- Walker, M.A., Schumacher, J., Schmitz, D.G., McMullen, W.C., Ruoff, W.W., Crabill, M.R., Hawkins, J.F., Hogan, P.M., McClure, S.R., Vacek, J.R., Edwards, J.F., Helman, R.G. and Frelief, P.F. (1998) Cobalt 60 radiotherapy for the treatment of squamous cell carcinoma of the nasal cavity and paranasal sinuses in three horses. *J. Am. vet. med. Ass.* **212**, 848-851.
- Walmsley, J.P. (1988) A case of atlanto-occipital arthropathy following guttural pouch mycosis in a horse. The use of radioisotope bone scanning as an aid to diagnosis. *Equine vet. J.* **20**, 219-220.
- Weller, R., Cauvin, E.R., Bowen, I.M. and May, S.A. (1999) Comparison of radiography, scintigraphy and ultrasonography in the diagnosis of a case of temporomandibular joint arthropathy in a horse. *Vet. Rec.* **144**, 377-379.
- Weller, R., Livesey, L., Maierl, J., Nuss, K., Bowen, I.M., Cauvin, E.R.J., Weaver, M., Schumacher, J. and May, S.A. (2001) Comparison of radiography and scintigraphy in the diagnosis of dental disorders in the horse. *Equine vet. J.* **33**, 49-58.